BELLCOMM, INC.
955 L'ENFANT PLAZA NORTH, S.W. WASHINGTON, D.C. 20024

B70 11049

SUBJECT: Subsatellite Attitude Determination
Case 310

DATE: November 20, 1970

FROM: W. O. Covington

ABSTRACT

The Particles and Fields subsatellite will be ejected from the Apollo 15 Service Module and spin stabilized at 12 RPM with its spin axis approximately normal to the ecliptic plane. The principal investigator for the magnetometer experiment desires that the spin axis of the subsatellite be maintained within 35° of the normal to the ecliptic plane for a period of one year and that the attitude of the spin axis be determined with an uncertainty of about one degree or less. It is desirable to determine the spin axis attitude using only the single sun aspect angle sensor currently included in the subsatellite design rather than to modify the design by adding another sensor.

A Kalman filter can be used to estimate the attitude of the satellite based on solar aspect angle measurements made periodically by the sun sensor on the subsatellite and telemetered to the ground for processing. The system dynamics, consisting of the precession of the satellite angular momentum vector in response to the lunar gravity gradient torque, is influenced indirectly by the anomalies in the lunar gravity field. The oblateness and higher order terms cause changes in the satellite orbital elements which in turn influence the gravity gradient torque. The analysis presented uses a computer statistical simulation of a Kalman filter attitude estimator.

The results indicate that the spin axis attitude can be estimated adequately using only an initial attitude estimate and sun aspect angle measurements made over a time period of about 60 days. In addition, the spin axis should remain acceptably close to the normal to the ecliptic plane.

BELLCOMM, INC.
955 L'ENFANT PLAZA NORTH, S.W. WASHINGTON, D. C. 20024

B70 11049

SUBJECT: Subsatellite Attitude Determination
Case 310

DATE: November 20, 1970

FROM: W. O. Covington

MEMORANDUM FOR FILE

1. INTRODUCTION

The Particles and Fields subsatellite will be ejected from the Apollo 15 Service Module and spin stabilized at 12 RPM with its spin axis approximately normal to the ecliptic plane. The subsatellite is a 14 inch diameter, 30 inch long prism with three 60 inch booms extending radially from one end of the prism. A magnetometer is mounted on the end of one of the booms.

The principal investigator for the magnetometer has two fundamental attitude requirements. First, he desires that the spin axis of the subsatellite be maintained within 35° (20° design goal) of the normal to the ecliptic plane for a period of one year. Second, he desires that the attitude of the magnetometer be determined with an uncertainty of about one degree or less.

It is desirable to determine the spin axis attitude using only the single sun aspect angle sensor currently included in the subsatellite design rather than to modify the design by adding another sensor. This sensor measures the angle between the satellite axis of symmetry and the line-of-sight to the sun. The ability to determine the spin axis attitude using only one sensor has been investigated and is reported in this memo.

After being ejected at 4 fps normal to the CSM orbit plane with spin axis aligned approximately normal to the ecliptic plane, gravity gradient torque acts on the spin-stabilized satellite causing its angular momentum vector to precess. If the lunar gravity field were spherical and the earth and sun were not present, the orbit plane would remain fixed in space, and the subsatellite angular momentum vector would precess about a normal to the orbit plane in a manner similar to the precession of the equinoxes of the earth. However, the non-spherical lunar gravity field and the gravity field of the earth cause changes in the elements of the subsatellite orbit which are manifested as changes in the orientation of the lunar gravity field with respect to the satellite

attitude. This effect influences substantially the gravity gradient torque acting on the satellite. To assure that magnetic and solar radiation pressure torques and earth and sun gravity gradient torques can be neglected, an estimate of the magnitude of these torques was made and compared with the magnitude of the lunar gravity gradient torque.

TRW has performed a study[1] of the spin axis precession rates with the moon modeled as an oblate spheroid and has concluded that the spin axis can be maintained within 35° to the normal to the ecliptic. Their study included various initial spin axis orientations and wedge angles between the ecliptic plane and the orbital plane. To verify the TRW conclusion, a few computer runs were made in this study with the moon modeled as an L-1 gravity field (currently used as the gravity model for Apollo missions) and including the effect of the Earth. However, the present study is most concerned with the ability to estimate accurately the attitude of the satellite based on sun sensor data.

2. ATTITUDE DETERMINATION

A Kalman filter can be used to estimate the attitude of the satellite based on solar aspect angle measurements made periodically by the sun sensor on the subsatellite and telemetered to the ground for processing. An estimate of the initial spin axis attitude along with an estimate of the measurement error can be used to improve the attitude estimate as sun angle data are received.

The magnitude of the gravity gradient torque acting on the satellite depends upon the difference between the spin axis moment of inertia and the transverse moment of inertia. The smaller this difference, the less will be the magnitude of gravity gradient torque. However, the difference cannot be reduced to zero since the satellite must have unequal moments of inertia for spin stabilization. TRW used a spin-axis-to-transverse moment of inertia ratio of 1.091 in their precession analysis, and this value was also used (with a spin axis moment of inertia of 1.4 slug ft^2) in this attitude determination analysis.[2]

The system dynamics, consisting of the precession of the satellite angular momentum vector in response to the lunar gravity gradient torque, is influenced indirectly by the anomalies in the lunar gravity field. The oblateness and the higher order terms cause changes in the satellite orbital

elements which in turn influence the gravity gradient torque. In the real-time filter, the orbital elements of the subsatellite will be estimated periodically from MSFN data. These frequently-updated elements can be used in the attitude filter, precluding the requirement for a highly accurate lunar gravity model.

The sun sensor, which measures the angle between the satellite axis of symmetry and a line-of-sight to the sun, consists of a photodetector and an aperture shaped to generate a 5 volt pulse of width 0.05 to 0.25 of a spin period, depending on the elevation of the sun above the satellite equatorial plane normal to the axis. Since the intensity threshold is set to respond to an illumination of 30% of solar intensity or greater, the earth and the moon produce no output. TRW estimates informally that the uncertainty in the sun angle measurement is approximately 1/2 degree.

The initial attitude of the satellite spin axis cannot be estimated during the first few days as accurately as the attitude later in time after much sun sensor data has been filtered. At this later time the accuracy of the initial attitude estimate can be greatly improved by integrating the current attitude estimate backward in time. This technique will permit early magnetometer data to be properly interpreted later in the mission after more sun angle measurements have been made.

3. COMPUTER SIMULATION

The analysis presented here uses a computer statistical simulation of a Kalman filter attitude estimator. A characteristic of the Kalman filter is that the estimated state error covariance matrix depends upon the initial value of this matrix, the estimated measurement error covariance matrix and the measurement schedule, and is independent of the actual measurements. This characteristic can be used to simulate the performance of the filter without actually making measurements. The results indicate the uncertainty in the attitude error assuming that the initial attitude error covariance matrix and the measurement error estimates used in the simulation correctly represent the corresponding real-world quantities and that the system dynamics model is valid.

A major question concerning the Kalman filter attitude estimator is: How long does the filter take to reduce the initial attitude estimate error to an acceptable value? The results of the analysis described in this memo provide an answer to this question.

The Kalman filter attitude estimator equations were developed as indicated in Appendix B. The state vector to be estimated is

$$X = \begin{bmatrix} \theta \\ \psi \end{bmatrix}$$

where θ, ψ are the orientation angles of the spin axis as shown in Fig. 1. The measured quantity is the angle, ϕ, between the subsatellite spin axis and the line-of-sight to the sun. Covariance matrix updates corresponding to measurement times were incorporated periodically each orbital revolution. The transition matrix used to propagate the state covariance matrix from one measurement time to the next was determined numerically as outlined in Appendix B. The fundamental filter equations used in the simulation were eq. (B-7) and (B-10) of Appendix B.

In this analysis it was assumed that the subsatellite is a rigid body spinning about its axis of symmetry. This assumption is realistic, since the wobble damper is designed to reduce the nutation of the satellite to less than 1/2 degree 26 hours after subsatellite deployment.

The precession rate equations for the subsatellite angular momentum vector were developed as indicated in Appendix A. A previously-developed[3] expression provided the average gravity gradient torque on the spin-stabilized satellite per orbital revolution. This average torque is a function of the orbital elements a, e, i, Ω as well as the satellite attitude and moments of inertia. A computer program was used to generate and tabulate the orbital elements as a function of time for the L-1 lunar gravity model[4] augmented with the effect of the earth's gravity. This element tableau was sampled periodically and interpolated to obtain elements for the gravity gradient torque expression. A computer program was used to integrate numerically the precession rate equations and to produce the orientation of the spin axis as a function of time. One orbital period was used as the integration interval, and the spin axis orientation angles were recorded at one day intervals.

The variances of the spherical coordinate angles θ and ψ cannot be added directly to yield a single-number

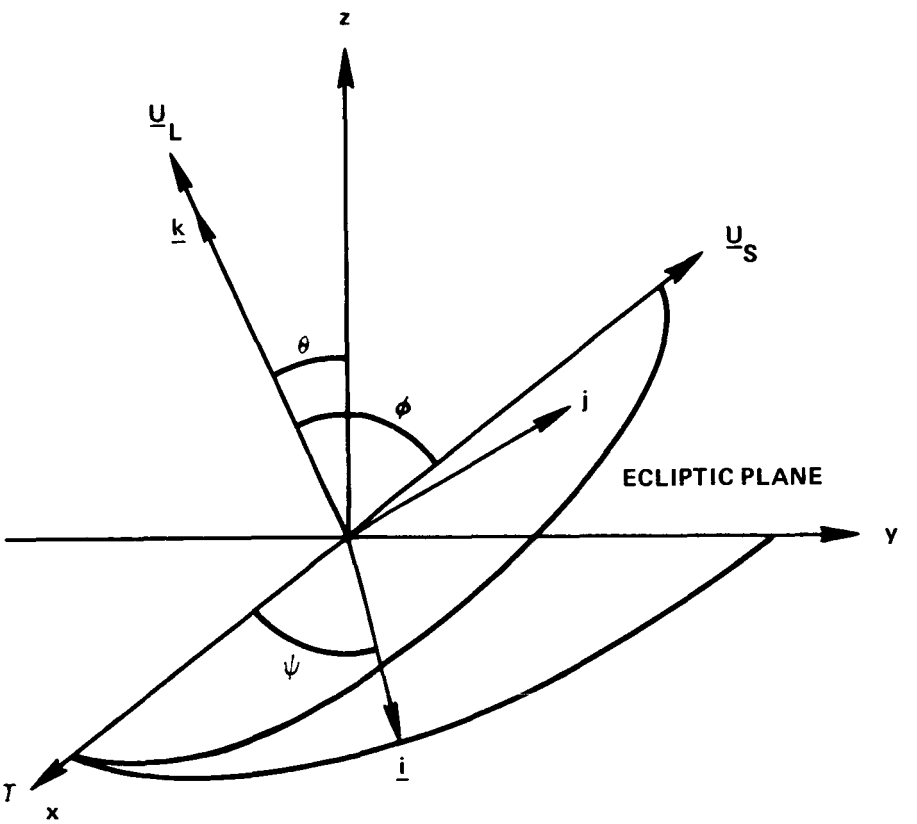

$\underline{U}_L$ = UNIT VECTOR ALONG SATELLITE ANGULAR MOMENTUM VECTOR

$\underline{U}_S$ = UNIT VECTOR ALONG DIRECTION TO SUN

x = VERNAL EQUINOX OF DATE
y = COMPLETES RIGHT-HAND SYSTEM
z = PARALLEL TO EARTH POLAR AXIS
$\underline{k}$ = UNIT VECTOR ALONG SPIN AXIS
$\underline{i}$,j = UNIT VECTORS COMPLETING RIGHT-HAND TRIAD

FIGURE 1 – GEOMETRY OF VECTORS.

variance for the attitude pointing error. The angles α and β defined in Appendix B are introduced to formulate a single-number attitude pointing error related to the state vector errors. The output of this simulation is the root-sum-square error angle

$$RSS = \sqrt{\sigma_\alpha^2 + \sigma_\beta^2}$$

where σ_α^2 = variance of angle α

σ_β^2 = variance of angle β

The relationship between the attitude error angles and errors in the state vector elements as developed in Appendix B are:

$$\delta\theta = \beta + \frac{\alpha^2}{2} \operatorname{ctn} \theta$$

$$\delta\psi = \frac{\alpha}{\sin \theta}$$

The non-linear term in the $\delta\theta$ expression is small when $\theta > 10°$ so that normally distributed errors remain approximately normally distributed through the transformation. (During this attitude determination simulation, $\theta > 18°$.) The standard deviations for the error angles are given by

$$\sigma_\theta = \sigma_\beta$$

$$\sigma_\psi = \frac{\sigma_\alpha}{\sin \theta}$$

which are the relationships used in the computer simulation.

The orbit used for the filter simulation was one considered typical of a J-mission. It was 60 NM altitude,

nearly circular, with ascending node and inclination equal to the third revolution of the Apollo 8 lunar orbit. The initial elements of the orbit were:

Ω = ascending node = -171.99°

i = inclination = 146.42°

a = semi-major axis = 6.066961924×10^6 ft.

e = eccentricity = 0.001

The filter simulation was initialized with an estimated state error covariance matrix corresponding to a pointing error apportioned equally in the α and β directions. Initial pointing errors of 5° and 10° were used, since these were representative of an available estimate of 8.07° by TRW.[1]

Several values of measurement error standard deviation between 0.1° and 2° were used to assess the effect of measurement error on the response time of the filter.

4. RESULTS

The RSS angle estimation error of the spin axis for several measurement sigmas is shown in Fig. 2 for an initial 10° attitude error apportioned equally between angles α and β. The first few measurements reduce the error in the measurement angle plane (plane of ϕ) but have little effect on the error normal to the measurement plane. Consequently, in Fig. 2 the RSS error is reduced from its initial 10° value to about 7° and remains there until the spin axis precession and the sunline movement yield a significant component of measurement angle normal to the original angle measurement plane.

The curves of Fig. 2 show the RSS estimation error for a σ = 0.5° measurement error, as estimated by TRW, along with several other curves for different performance. The curves show that a measurement interval of 30 to 90 days will be required to reduce an initial ten degree attitude uncertainty to a value less than 1°, depending upon the accuracy of the measurements.

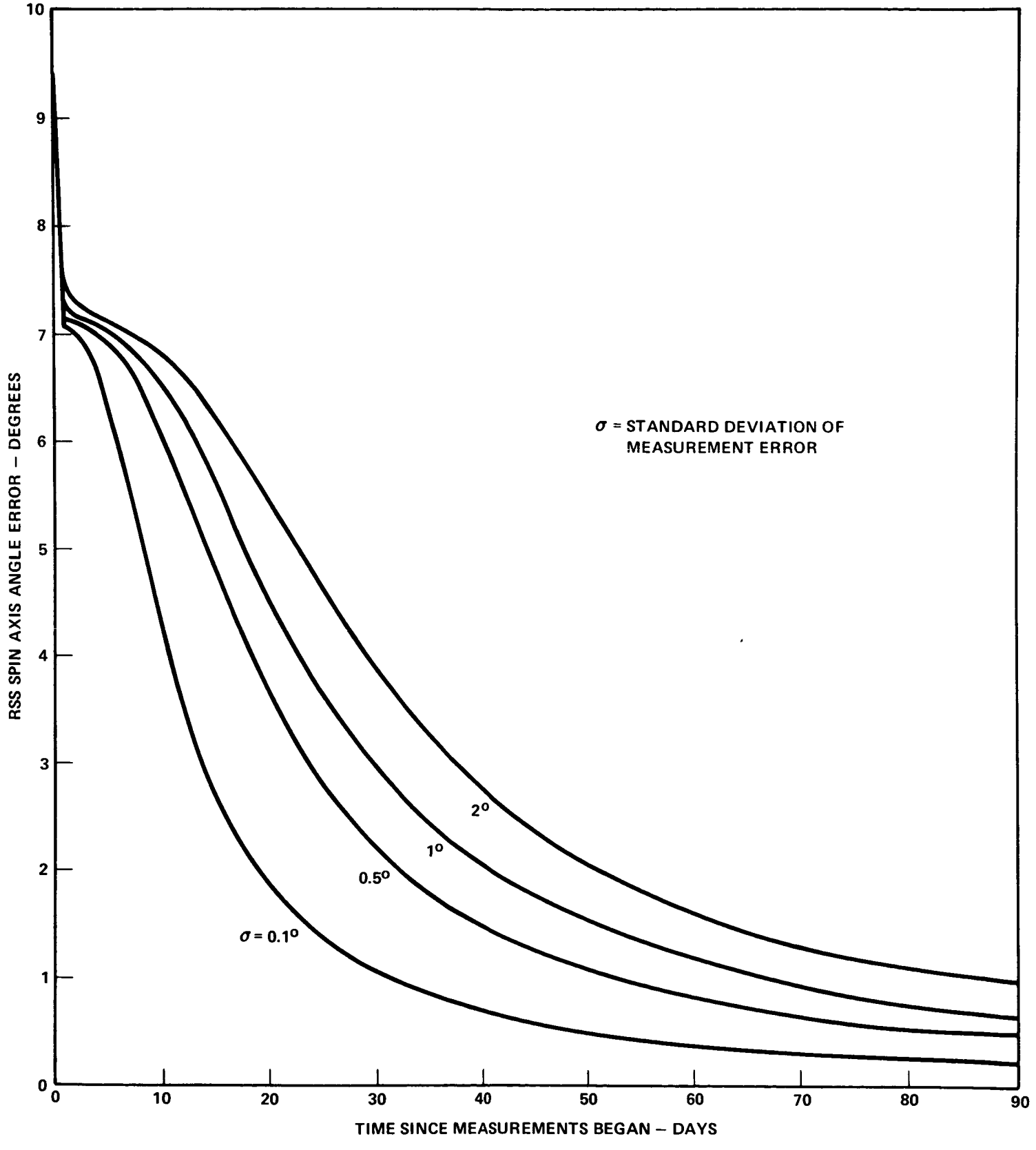

FIGURE 2 – ESTIMATED SPIN AXIS ATTITUDE ERROR FOR 10° INITIAL ERROR.

The effect of the initial attitude estimate error can be seen by comparing the curves of Fig. 3 for an initial error of 5 degrees with corresponding curves of Fig. 2 for 10 degrees. In both cases the error is not reduced below 1 degree until 30 to 90 days have elapsed permitting measurements normal to the original measurement angle plane. This result shows that there is little benefit in attempting to measure the initial attitude by photographic or other means unless the associated error is within the acceptable range of about 1 degree. An initial measurement which reduces the initial attitude error from 10° to 5° does not significantly reduce the response time of the filter.

A few runs were made to verify TRW's conclusion that the spin axis of the subsatellite can be maintained within the required 35° of a normal to the ecliptic during a one-year time period for wedge angles as large as 45° between the orbital plane and the ecliptic. The deviation of the spin axis from the normal to the ecliptic plane is shown in Fig. 4 for a representative J-mission orbit and for a highly-inclined orbit. The representative orbit produced a maximum deviation angle less than 7°. The highly-inclined orbit (45° wedge angle between orbit plane and ecliptic plane) yields a maximum deviation of the spin axis from the normal to the ecliptic of 21.7°, which is well within the required 35° limit.

5. CONCLUSION

These results indicate that the spin axis attitude of the subsatellite can be estimated adequately using only an initial attitude estimate and sun aspect angle measurements made over a time period of about 60 days. Early attitude history of the satellite can be obtained by integrating current spin axis orientation estimates backward in time. In addition, the spin axis should remain acceptably close to the normal to the ecliptic plane.

2014-WOC-ksc

W. O. Covington

Attachments
Appendix A and B

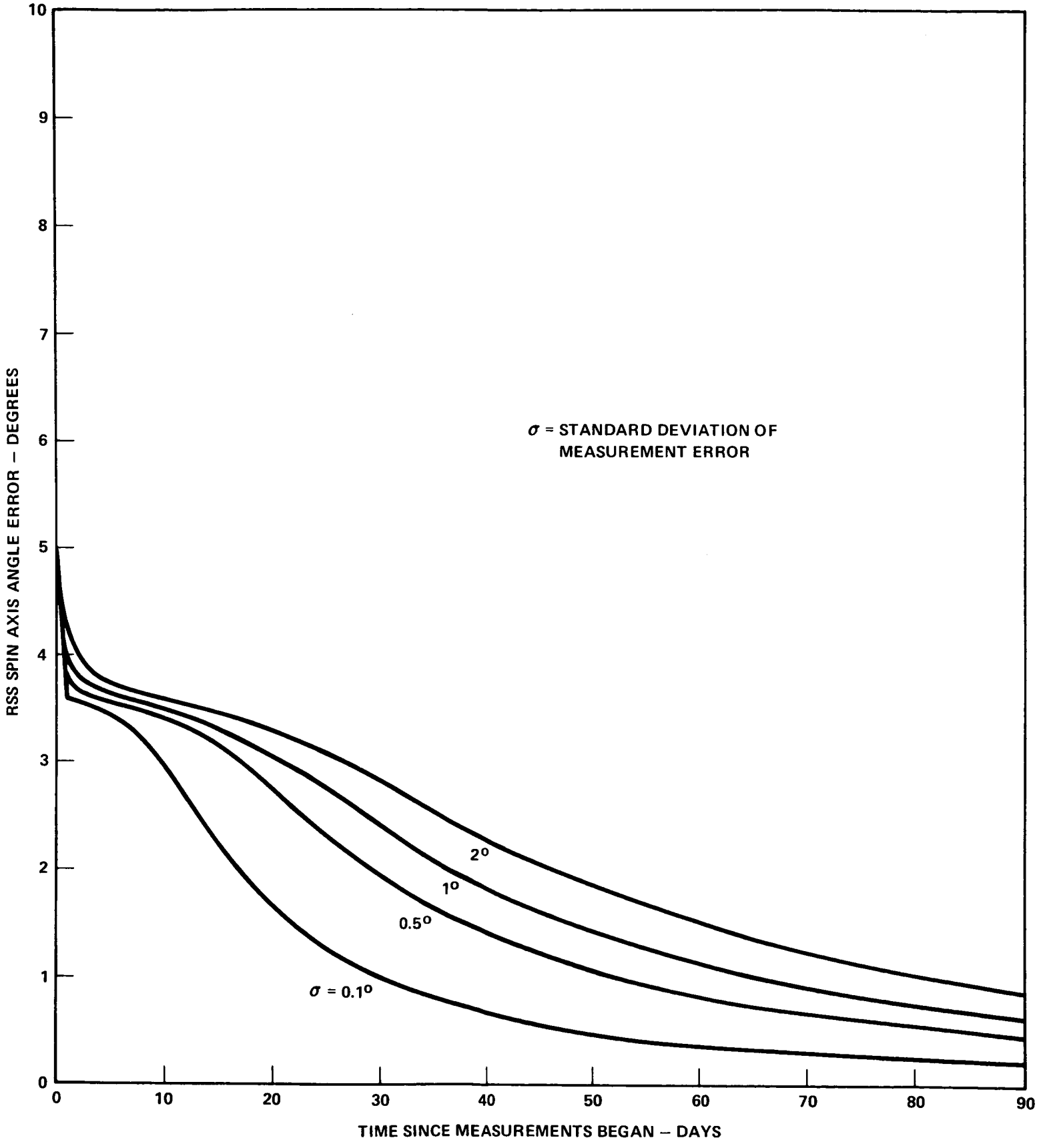

FIGURE 3 – SPIN AXIS ATTITUDE ERROR FOR 5° INITIAL ERROR.

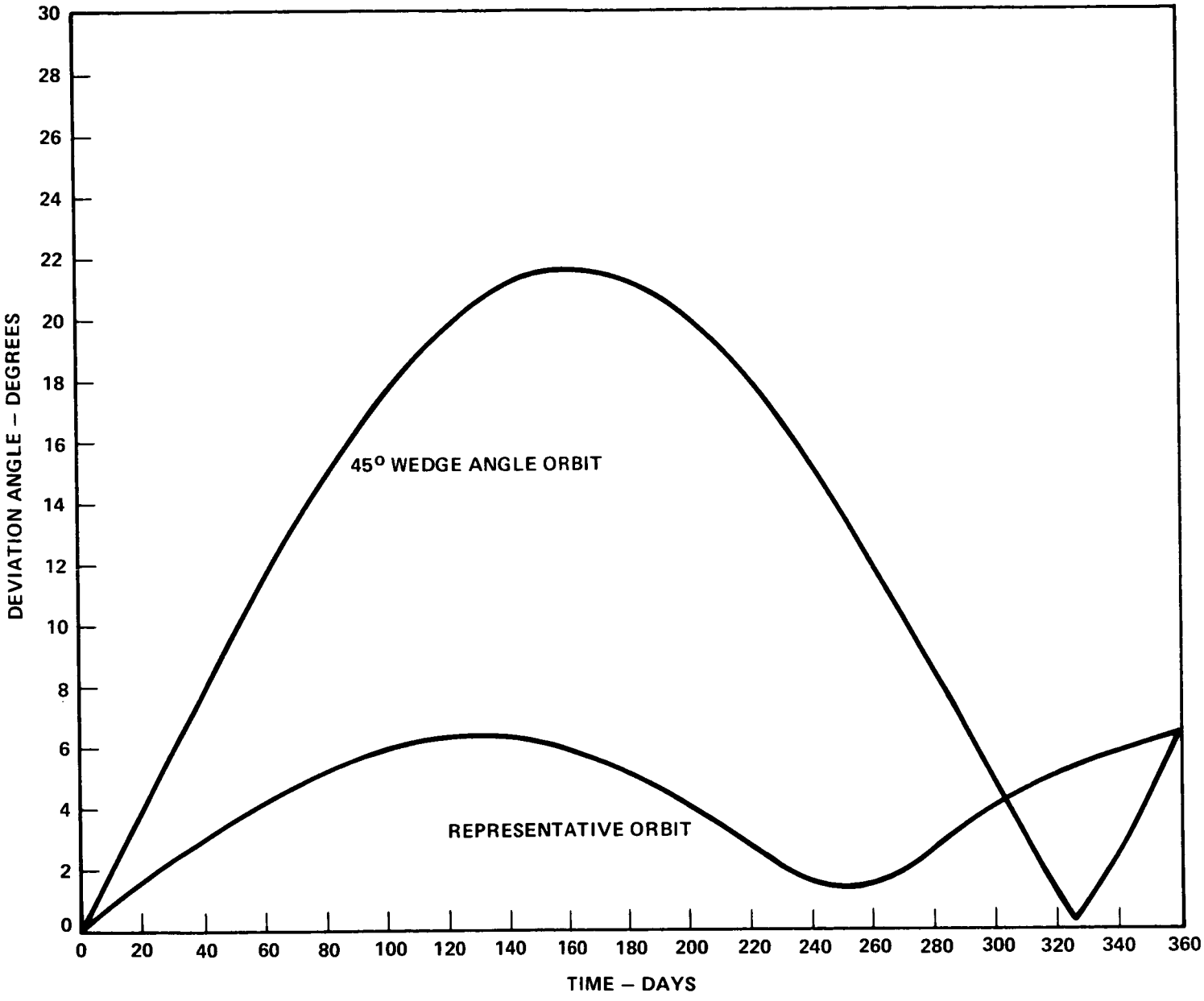

FIGURE 4 – SPIN AXIS DEVIATION FROM NORMAL TO ECLIPTIC.

REFERENCES

1. "Dynamics Subsystem Critical Design Review Package", TRW Systems Group, July 14-15, 1970.

2. "Proposal for a Particles and Fields Subsatellite for the Apollo Lunar Program", TRW Systems Group, March 1970.

3. Thomas, L. C. and Cappellari, J. O.; "Attitude Determination and Prediction of Spin-Stabilized Satellites," Bell System Technical Journal, July 1964.

4. Wollenhaupt, W. R.; "Apollo Orbit Determination and Navigation", AIAA 8th Aerospace Sciences Meeting, January 1970.

5. Roberson, Robert E., "Gravitational Torque on a Satellite Vehicle", Journal of the Franklin Institute, January 1958.

6. Bryson and Ho, Applied Optional Control, Blaisdell, 1969.

Appendix A

Development of Precession Rate Equations

The orientation of the subsatellite momentum vector is described by the angles θ and ψ in the selenocentric inertial coordinate system shown in Fig. A-1. The unit vector along the momentum vector is

$$\underline{u}_L = \underline{e}_1 \sin\theta \sin\psi - \underline{e}_2 \sin\theta \cos\psi + \underline{e}_3 \cos\theta$$

The gravity gradient torque will be described in terms of the $\underline{i}$, $\underline{j}$, $\underline{k}$ right-hand, orthogonal unit vectors where $\underline{k}$ lies along $\underline{u}_L$ and $\underline{i}$ lies in the xy plane. The rotation-dynamics equation is:

$$\underline{N} = \dot{\underline{L}} = \underline{b}_i \dot{L}_i + \underline{\Omega} \times \underline{L} \qquad \text{(A-1)}$$

where

$\underline{N}$ = torque vector

$\underline{L}$ = angular momentum vector

$\underline{b}_i$ = unit base vectors in satellite body axes

$\dot{L}_i$ = components of rate of change of the magnitude of the satellite momentum vector

$\underline{\Omega}$ = satellite angular velocity vector

Since the satellite spin rate is assumed constant, the magnitude of $\underline{L}$ is constant, $\dot{L}_i = 0$ and eq. (A-1) reduces to

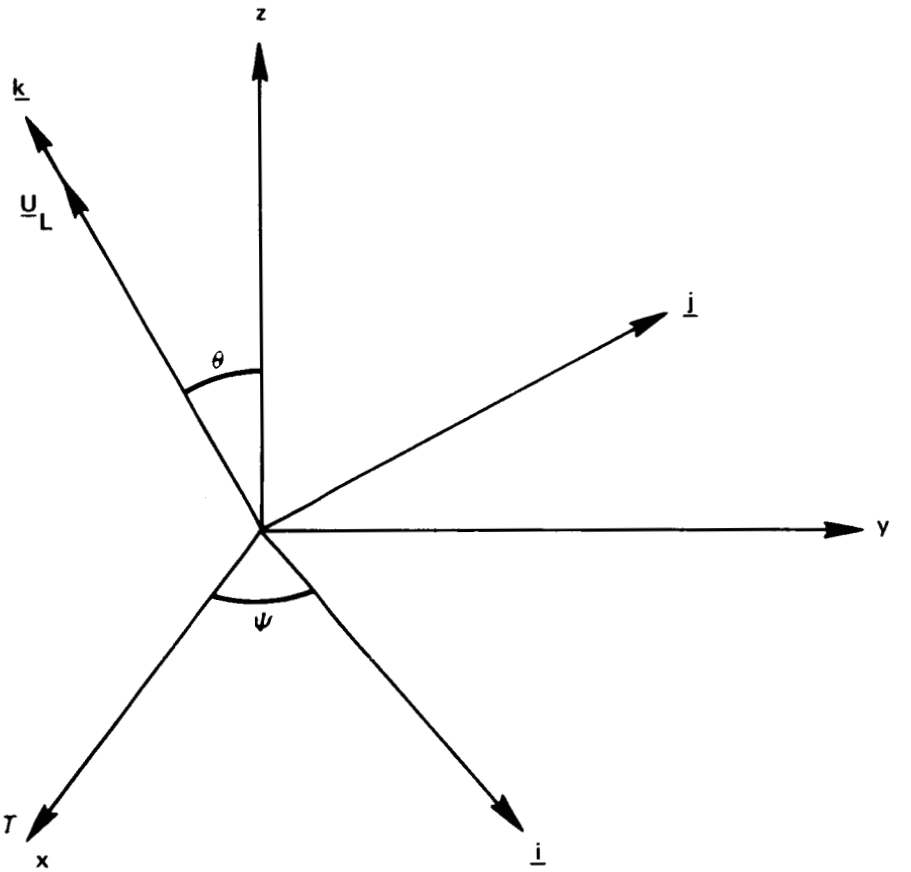

x : TO VERNAL EQUINOX OF DATE
y : COMPLETES RIGHT HAND SYSTEM
z : PARALLEL TO EARTH POLAR AXIS

$\underline{U}_L$ = UNIT VECTOR ALONG SUBSATELLITE ANGULAR MOMENTUM VECTOR

FIGURE A-1 – DEFINITION OF SPIN AXIS ORIENTATION VECTOR.

$$\underline{N} = \underline{\Omega} \times \underline{L} \tag{A-2}$$

where

$$\underline{\Omega} = \underline{i}\dot{\theta} + \underline{j}\dot{\psi} \sin\theta + \underline{k}\dot{\psi} \cos\theta \tag{A-3}$$

$$\underline{L} = \underline{k}L \tag{A-4}$$

The gravity gradient torque arises principally from the spherical portion of the gravity field. The effect of oblateness is of the order of J_{20} of the spherical field, where J_{20} is the first zonal harmonic.[5] For the lunar field $J_{20} = 2.071 \times 10^{-4}$, so that the oblateness effect on the gravity gradient torque will be neglected. Higher harmonic terms of the lunar gravity field will also be neglected since their individual effect on the gravity gradient torque will be smaller than the oblateness term and since their combined effect is not likely to produce reinforcement.

The torques due to the earth and the sun gravity gradients and to the magnetic moment are also small. Estimates of the maximum instantaneous magnitudes of these torques relative to the maximum instantaneous magnitude of the lunar gravity gradient are:

Earth Gravity Gradient: 10^{-5}

Sun Gravity Gradient: 10^{-8}

Magnetic Moment: 10^{-8}

The maximum magnitude of the torque due to the solar radiation pressure as estimated with available vehicle data is of the order of 5% of the maximum lunar gravity gradient torque. This relatively large estimate and the uncertainty in the estimate suggest that special vehicle design may be required to suppress the solar radiation torque. Accurate estimates of this torque must await the availability of center of gravity location information and the kinds and distributions of surface coatings.

The gravity gradient torque on the satellite averaged over one period is[3]

$$\underline{N} = F\{[\sin i \cos\theta \cos(\Omega-\psi) - \cos i \sin\theta]\underline{i} + \sin i \sin(\Omega-\psi)\underline{j}\} \quad \text{(A-5)}$$

where

$$F = \frac{6\pi^2(I_3-I)}{T_n^2(1-e^2)^{3/2}} [\cos i \cos\theta + \sin i \sin\theta \cos(\Omega-\psi)]$$

I_3 = moment of inertia of satellite about its spin axis

I = moment of inertia transverse to spin axis

T_n = period of orbit

e = eccentricity

i = inclination of orbit

Ω = ascending node of orbit

Substituting eqs. (A-3), (A-4), (A-5) into (A-2), the precession rates are given by

$$\dot{\psi} = \frac{F}{L\sin\theta} [\sin i \cos\theta \cos(\Omega-\psi) - \cos i \sin\theta] \quad \text{(A-6)}$$

$$\dot{\theta} = -\frac{F}{L} \sin i \sin(\Omega-\psi) \quad \text{(A-7)}$$

These angular rates are numerically integrated in the computer program to produce the satellite spin axis Euler angles.

Appendix B

Development of Kalman Filter Attitude Estimator Equations

The system is modeled as a state equation and a measurement relation.

$$\dot{\underline{x}} = f(\underline{L}, \underline{N}) \tag{B-1}$$

$$\phi = \phi(\underline{x}, \underline{u}_s, \nu) \tag{B-2}$$

where:

$\underline{x} = \begin{bmatrix} \theta \\ \psi \end{bmatrix}$ = state vector

ϕ = measured solar aspect angle (angle between vehicle axis of symmetry and the direction to the sun)

$\underline{u}_s$ = unit vector directed toward sun

ν = white, Gaussian measurement noise

$\underline{L}$, $\underline{N}$ defined in Appendix A

Eq. (B-1) is given by eqs. (A-6) and (A-7). The measurement relation can be developed from the vectors of Fig. B-1. The unit vector along the spin axis of the satellite is given by

$$\underline{u}_L = \underline{e}_1 \sin\theta \sin\psi - \underline{e}_2 \sin\theta \cos\psi + \underline{e}_3 \cos\theta \tag{B-3}$$

The unit vector normal to the ecliptic is

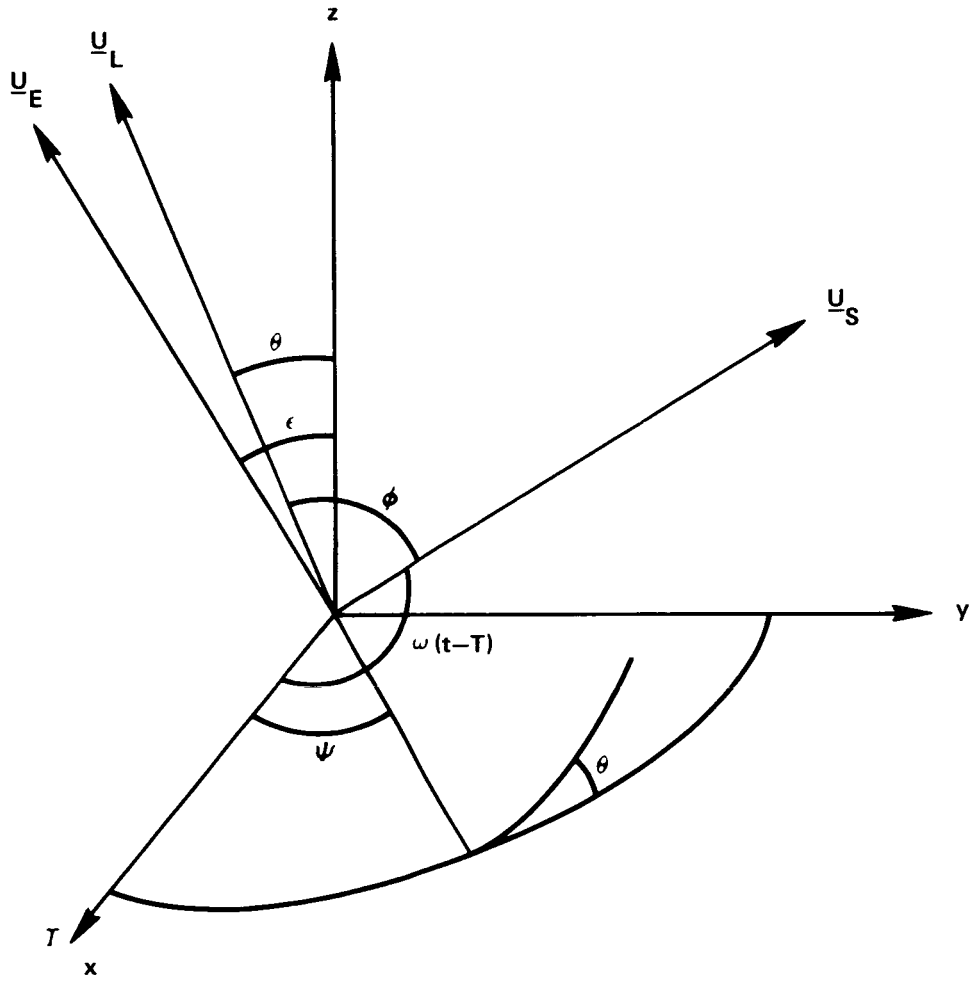

$\underline{e}_1, \underline{e}_2, \underline{e}_3$ = UNIT VECTORS IN SELENOCENTRIC INERTIAL COORDINATES

$\underline{U}_E$ = UNIT VECTOR NORMAL TO ECLIPTIC PLANE

$\underline{U}_L$ = UNIT VECTOR ALONG SATELLITE ANGULAR MOMENTUM VECTOR, $\underline{L}$

$\underline{U}_S$ = UNIT VECTOR ALONG DIRECTION TO SUN

FIGURE B-1 – GEOMETRY OF VECTORS FOR ATTITUDE ESTIMATION.

$$\underline{u}_E = -\underline{e}_2 \sin\varepsilon + \underline{e}_3 \cos\varepsilon \qquad \text{(B-4)}$$

where ε = obliquity of the ecliptic $\approx 23.45°$. For the present analysis the unit vector directed toward the sun will be developed in terms of the mean orbital rate of the earth about the sun. In the real-time filter, however, the sun direction vector determined by precise astronomical measurements would, of course, be used. This simplification for this analysis is justified since no estimate of attitude is made based on experimental data. The unit vector directed toward the sun is normal to $\underline{u}_E$ and is given by

$$\underline{u}_s = \underline{e}_1 \cos\omega(t-T) + \underline{e}_2 \sin\omega(t-T) \cos\varepsilon + \underline{e}_3 \sin\omega(t-T) \sin\varepsilon \qquad \text{(B-5)}$$

where ω = mean orbital rate of the earth about the sun

$t-T$ = time since vernal equinox

T = time of vernal equinox

The cosine of the measured sun aspect angle is given by

$$\cos\phi = \underline{u}_L \cdot \underline{u}_s$$

$$\cos\phi = \sin\theta \sin\psi \cos\omega(t-T) - \sin\theta \cos\psi \sin\omega(t-T) \cos\varepsilon + \qquad \text{(B-6)}$$

$$+ \cos\theta \sin\omega(t-T) \sin\varepsilon$$

The Kalman filter equations have been described in numerous places and are given by[6]

$$\hat{E}_+^{-1} = \hat{E}_-^{-1} + H\hat{Q}^{-1} H^T \qquad \text{(B-7)}$$

$$W = \hat{E}_+ H \hat{Q}^{-1} \tag{B-8}$$

$$\hat{\underline{x}}_+ = \hat{\underline{x}}_- + W(\tilde{\phi} - \hat{\phi}) \tag{B-9}$$

$$\hat{E}_- = \hat{E}_n' = \Phi_{n,\,n-1}\, \hat{E}_{n-1}\, \Phi_{n,\,n-1}^T \tag{B-10}$$

where $\underline{x}$ = state vector

ϕ = measurement vector (scalar in this case)

$H^T = \left[\frac{\partial \phi}{\partial \theta}, \frac{\partial \phi}{\partial \psi} \right]$

$\hat{E}$ = estimated covariance matrix of $\underline{x}$

$\hat{E}_- = \hat{E}_n'$ = estimated covariance matrix after propagation by transition matrix and prior to incorporation of measurement data

$\hat{E}_+$ = estimated covariance matrix after incorporation of measurement data

$\hat{Q}$ = estimated covariance matrix of ϕ (simply the estimated variance of ϕ in this case, since ϕ is a scalar)

$\Phi_{n,\,n-1}$ = transition matrix of $\underline{x}$

W = filter weighting matrix, which minimizes the trace of $\hat{E}_+$

The elements of H are derived from eq. (B-6) as

$$\frac{\partial \phi}{\partial \theta} = -\frac{1}{\sin\phi} (C_1 \cos\theta \sin\psi - C_2 \cos\theta \cos\psi - C_3 \sin\theta) \tag{B-11}$$

$$\frac{\partial \phi}{\partial \psi} = -\frac{1}{\sin\phi} (C_1 \sin\theta \cos\psi + C_2 \sin\theta \sin\psi) \tag{B-12}$$

where $C_1 = \cos\omega(t-T)$

$C_2 = \sin\omega(t-T)\ \cos\varepsilon$

$C_3 = \sin\omega(t-T)\ \sin\varepsilon$

In the present analysis, eq. (B-10) was used to propagate the covariance matrix between measurement points, and eq. (B-7) was used to update the covariance matrix at measurement points. The results expressed in terms of orientation angular errors correspond to correctly estimated initial state error and measurement error and to a valid system model.

The spin axis orientation error can be expressed as the root-sum-square of the α and β error components defined in Fig. B-2. The computed attitude error is

$$RSS = \sqrt{\sigma_\alpha^2+\sigma_\beta^2} = \sqrt{\sigma_\psi^2\ \sin\theta^2+\sigma_\theta^2}$$

where σ_α^2, σ_β^2 = variances of α, β respectively.

These α and β angles are introduced to generate a single-number attitude error estimate for this analysis. The real-time filter would simply have the attitude error estimates stored in the $\hat{E}$ covariance matrix.

The transition matrix for vector $\underline{x}$ must be determined from eq. (B-1): This non-linear equation would yield rather lengthy expressions in linearized form. An alternative is to compute the transition matrix numerically by injecting small variations in the state vector elements, numerically integrating eq. (B-1) and differencing the result produced at the later time. This alternative, which was used in this analysis, provided the transition matrix as follows:

$$\Phi_{n,\ n-1} = \begin{bmatrix} \Phi_{11} & \Phi_{12} \\ \Phi_{21} & \Phi_{22} \end{bmatrix}$$

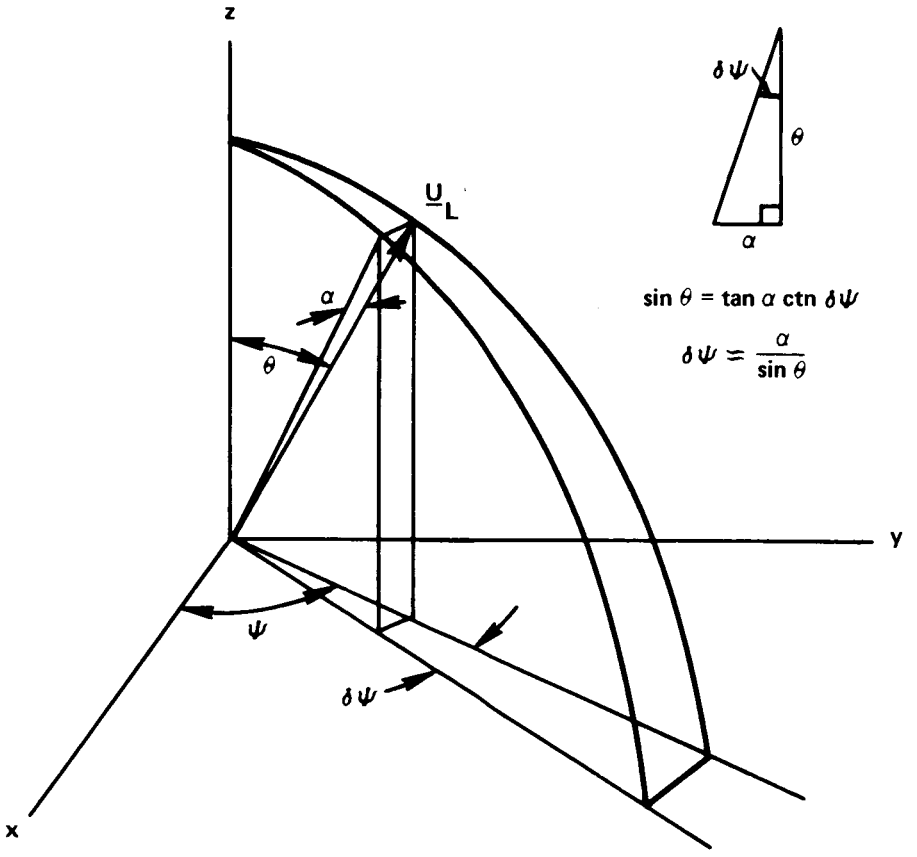

$\underline{U}_L$ = UNIT VECTOR ALONG SATELLITE SPIN AXIS

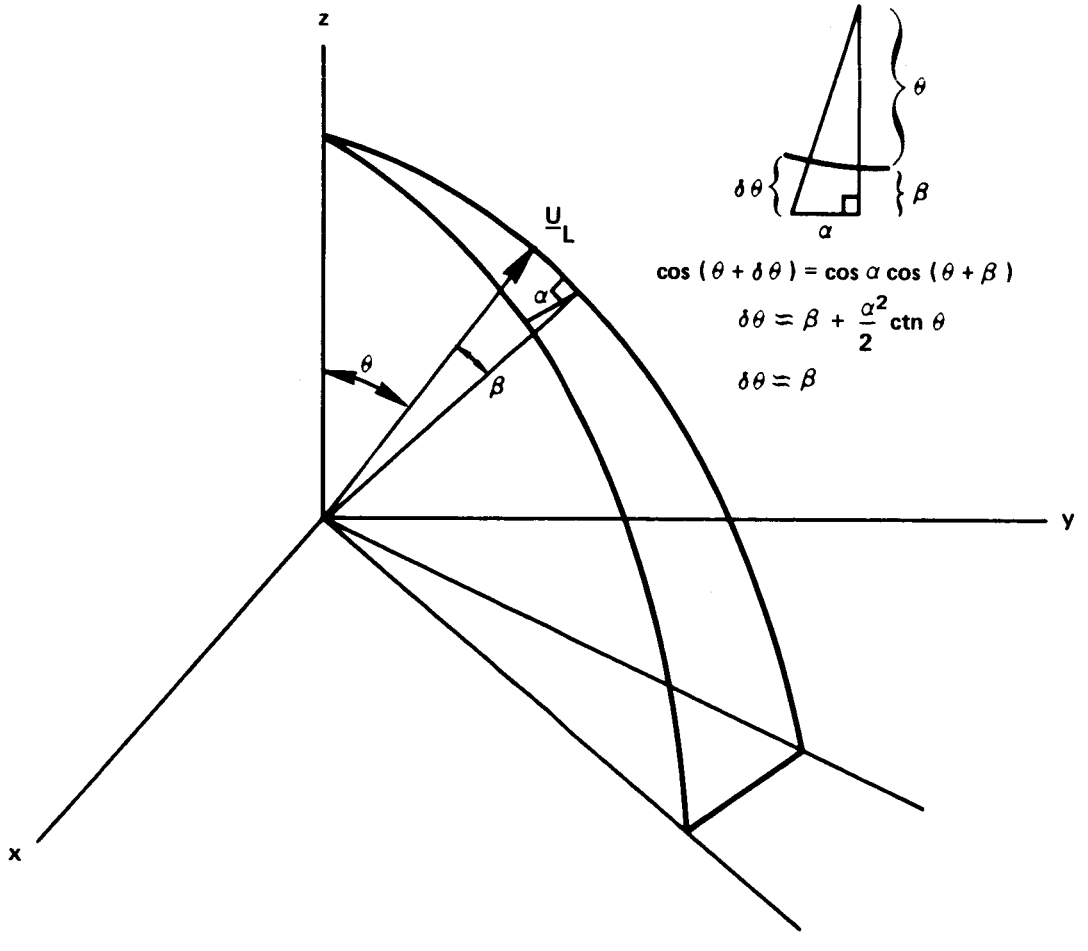

FIGURE B-2 – DEFINITION OF ATTITUDE ERROR ANGLES.

where

$$\Phi_{11} = \frac{\theta_n(\theta_{n-1}+\Delta\theta,\ \psi_{n-1}) - \theta_n(\theta_{n-1},\ \psi_{n-1})}{\Delta\theta}$$

$$\Phi_{12} = \frac{\theta_n(\theta_{n-1},\ \psi_{n-1}+\Delta\psi) - \theta_n(\theta_{n-1},\ \psi_{n-1})}{\Delta\psi}$$

$$\Phi_{21} = \frac{\psi_n(\theta_{n-1}+\Delta\theta,\ \psi_{n-1}) - \psi_n(\theta_{n-1},\ \psi_{n-1})}{\Delta\theta}$$

$$\Phi_{22} = \frac{\psi_n(\theta_{n-1},\ \psi_{n-1}+\Delta\psi) - \psi_n(\theta_{n-1},\ \psi_{n-1})}{\Delta\psi}$$

These expressions were used with $\Delta\theta$, $\Delta\psi = 1/2°$ in the computer program to generate the transition matrix.

BELLCOMM, INC.

Subject: Subsatellite Attitude Determination

From: W. O. Covington

DISTRIBUTION LIST

Complete Memorandum to

NASA Headquarters

J. K. Holcomb/MAO
E. W. Land, Jr./MAO
C. M. Lee/MA
A. S. Lyman/MR
R. A. Petrone/MA
W. E. Stoney/MAE

Manned Spacecraft Center

A. J. Calio/TA
K. J. Cox/EG23
J. H. Johnson/EE17
E. M. Jones/EG26
K. L. Lindsay/EG23

Jet Propulsion Laboratory

W. Sjogren

TRW

R. A. Browne
R. Gluck
T. Pederson
M. P. Scher

UCLA

P. Coleman

Complete Memorandum to

Bellcomm, Inc.

D. R. Anselmo
A. P. Boysen, Jr.
J. O. Cappellari, Jr.
D. A. Corey
D. A. De Graaf
F. El-Baz
D. R. Hagner
W. G. Heffron
J. J. Hibbert
P. J. Hickson
N. W. Hinners
T. B. Hoekstra
M. Liwshitz
J. L. Marshall
K. E. Martersteck
J. Z. Menard
W. L. Piotrowski
P. E. Reynolds
W. R. Sill
R. V. Sperry
J. W. Timko
R. L. Wagner
A. G. Weygand
W. D. Wynn
Department 1024 File
Central Files
Library

Abstract Only to

Bellcomm, Inc.

J. P. Downs
I. M. Ross
M. P. Wilson